Numerical Study on the Transient Response of a Condenser Microphone

Akbar Ranjbar, Mohammad Taghi Mehrabani, and Fatameh Torkaman Pary

***Abstract*— The vibrating of a condenser microphone diaphragm due to incident pressure causes changes in the capacitance and the energy stored in the volume of the microphone. One of the most important parameters that must be determined very precisely for any microphone is the amount of this displacement due to the executed pressure on the diaphragm i.e., mechanical sensitivity. Thus, in this paper, the generalized equations describing the motion of the diaphragm and the Reynolds equation for compressible gases have been solved in transient mode to determine with precision the mechanical response of the microphone. Unlike the past static and quasi dynamic simulations, the Reynolds equation that is used to calculate the damping and stiffness of the air near the diaphragm is considered in nonlinear form. The numerical frequency response obtained for a condenser microphone has been compared with experimental results that exist in the literature. The numerical results obtained indicate a very good accuracy of the code. The effect of the damping and stiffness coefficient on the frequency range, which is very important in designing a practical microphone, is also studied in detail. Such a dynamic analysis, unlike the past numerical static simulation, gives a deeper view into the reasons of the nonlinearity of this important measuring transducer.**

***Index Terms*— Condenser microphone, squeeze film, transient response.**

NOMENCLATURE

a	Radius of the microphone diaphragm.
Σ	Mass surface density of the diaphragm.
x	First Cartesian coordinate.
y	Second Cartesian coordinate.
x_{hole}	x of center of the holes.
y_{hole}	y of center of the holes.
r	First polar coordinate.
θ	Second polar coordinate.
h_0	Electrode gap distance.
y	Diaphragm deflection.
h	Sum of electrodes polarized gap distance and diaphragm deflection.
p_b	Back volume pressure.
b	Back plate radius.
u	Velocity along the holes.
ε_0	Permittivity of the air.
E_0	Polarization voltage.
T	Diaphragm tension.
p_i	Incidence pressure.
t	Time variable.
p	Local pressure.
p_0	Ambient pressure.
V_z	Normal velocity of the diaphragm.
h^*	Polarized gap.
V_{ave}	Average velocity of the diaphragm.
P_{ave}	Average pressure over the back plate.
υ_h	Scale velocity of the flow inside the channels.
r_{hole}	Radius of the holes.
γ	Atomic coefficient.
V_b	Back volume.
f_h	Vacuum resonance frequency.
y_h	Distribution function of holes and slots.
dm/dt	Mass flux of the flow through the channels.
h_d	Scale deflection of the diaphragm.
τ	Period of the incidence pressure.
X_d	Developing length.
D_h	Diameter of the holes.
ρ	Density of the fluid.
p_e	Electrostatic pressure on the diaphragm due to polarization voltage.
Y_0	Maximum center deflection of diaphragm in static manner.
M_e	Mechanical transfer function.
r_h	Holes radius.
l_h	Holes length.
l_{slot}	Slot length.
R	Ring radius.
θ_0	Start angle for the holes pattern.

GREEK SYMBOLS

μ	Ave.

Manuscript received August 8, 2011; revised February 11, 2012; accepted February 28, 2012. Date of publication March 6, 2012; date of current version June 6, 2012. The associate editor coordinating the review of this paper and approving it for publication was Prof. Okyay Kaynak.

A. Ranjbar is with the Electrical Engineering Department, Shahed University, Tehran 3319118651, Iran (e-mail: ranjbar@shahed.ac.ir).

M. T. Mehrabani and F. Torkaman Pary are with the Acoustic Laboratories, Shahed University, Tehran 3319118651, Iran (e-mail: mehrabani@aut.ac.ir; torkaman@shahed.ac.ir).

Color versions of one or more of the figures in this paper are available online at http://ieeexplore.ieee.org.

Digital Object Identifier 10.1109/JSEN.2012.2190055

I. INTRODUCTION

CONDENSER microphones are known to posses very low levels of nonlinear distortions for moderate sound pressure levels. This property has lead to their wide application such as measuring microphones. As the measured

sound pressure levels become larger, the level of nonlinear distortions increases. The non-uniform deflection of the microphone diaphragm causes a nonlinear relationship between the deflection of the diaphragm and the induced voltage.

In condenser microphones the sound pressure impinging on its flexible diaphragm causes diaphragm deflection which in turn changes the capacitance between the diaphragm and the rigid back plate. The changes in the capacitance are then converted to a voltage signal in an electrical circuit connected into the diaphragm and the back plate. Since the electric force in the capacitor is always attractive, a bias voltage source is used in this circuit to maintain the potential difference between the diaphragm and the back plate. In this complex acoustical electromechanical system, which consists of tightly coupled acoustical, electrical, and mechanical elements, a common modeling approach to evaluate the microphone performance is the lumped-element method [1, 2]. In this method, via simple analytical expressions, mass, compliance, and damping have their equivalent electrical counterparts in inductance, capacitance, and resistance, respectively. These parameters are usually calculated using the Squeeze Film Theory but with lots of simplification such as ignoring the holes pattern on the back plate [3]. Another modeling approach is the finite element method [4] that simulates a 3D flow of the air between the electrodes and through the holes with huge computational costs. An accurate but more complicated modeling approach has been described by Zuckerwar [5, 6] and verified with very good accuracy. This approach also provides an accurate expression for the air resistance term due to mechanical losses in the air gap, slot, and holes. Besides having all these advantages, this modeling cannot take into account the effect of the non-circular holes and slot on the back plate. Recently Ranjbar and Mehrabani [7] developed a new modeling approach to simulate the mechanical response of the microphone, using the Linear Squeeze Film Theory. Although this method was simple but it did not include the compressibility of the fluid between the electrodes.

The natural vibration of the diaphragm within the operating frequency range of the microphone can cause distortion in the output signal and hence, a vibration analysis of the diaphragm in the presence of the electric field is essential in the microphone design. The bias voltage between the diaphragm and the back plate can be considered as a constant for such vibration analysis [8, 9].

The electric field, due to the constant bias voltage, introduces a load intensity which increases with the diaphragm deflection. The influence of the electrostatic field on the static and dynamic deflection of circular diaphragm was studied by Warren et al [10, 11] using numerical techniques. In this dynamic deflection analysis, they used an approximate thin air film model developed by Hayasaka [12] to relate the reaction pressure of the air in the gap to the dynamic defection. A central difference numerical approach was then used to solve the coupled differential equations for the diaphragm and the air in the gap. The damping effect of air layer between the two electrodes was estimated by Chen by solving a simplified one- dimensional Reynolds equation in the Squeeze Film Theory [13]. Instead of considering a different holes pattern on the back plate it was assumed that all the holes gathered in the center of back plate and that consequently there is only one hole with the same area as all the holes. Huang examined the effect of flow around a diaphragm while it was vibrating. He presented a linear analysis of the coupling between the Poiseuille flow and a tensioned diaphragm of finite length using an Eigen value approach [14].

The vibration of a rectangular microphone diaphragm in the presence of electrostatic field was studied in reference [15] using the Rayleigh-Ritz method after linearizing the nonlinear effects of the electrostatic field. While the assumed deflection shape accounted for the dynamic deflection only the non-homogeneous terms resulting from the Rayleigh Ritz procedure on the linearized problem was also disregarded. The influence of diaphragm stability and vibration on a condenser microphone was examined in [16]. The analysis shows that as the field strength increases, the steady defection also increases and reaches a neutral equilibrium state corresponding to a critical value of the field strength. Any further increase in the field strength buckles the diaphragm on to the back plate.

A nodal analysis model of a condenser microphone has been implemented in an IC design environment. The fundamental characteristics, including sensitivity, frequency response and output referred noise are obtained by co-simulation with the microphone and the readout circuit using the Cadence simulator [17].

This paper presents a numerical analysis carried out with the second order finite difference method (FDM) in order to determine precisely the nonlinearity between the incidence pressure and the diaphragm deflection. To do so, first the unsteady equation of motion of a circular diaphragm is proposed and a numerical procedure to determine whether the air gap pressure has been presented. For this purpose, the Squeeze Film Theory (Reynolds equation) has been explained in an unsteady state and unlike the past estimations of the pressure by an analytical solution such as that of Reynolds which did not include the effects of the holes pattern, in this simulation the dependence of the air damping to the geometry of back plate such as air gap, holes pattern, holes diameter, number of holes and the diaphragm deflection shape are studied numerically.

The diaphragm is considered as a thin circular plate clamped at its periphery. Further, the differential equation of the plate is solved directly in order to examine the non-linear behavior and stability of the system. By coupling the vibration equation of the diaphragm, the Reynolds equation and the pressure rate for back volume, it is possible to determine the mechanical response of the microphone precisely. This new method is much easier than the previous analytical method which exists in the literature and can be used for any diaphragm shape, holes pattern and holes shape.

II. Governing Equation

The most important part of a condenser microphone simulation is based on modeling the microphone diaphragm vibration. To do so in the following section (2.1) the general equation of the diaphragm motion is proposed and explained and then in section (2.2), for the pressure distribution simulation between the two electrodes, the squeeze film theory has

been explained. The numerical way to determine the damping pressure is discussed in section (3). The method to consider the holes on the back plate to reduce the overall pressure has been also described.

A. Diaphragm Equation of Motion

Transient vibrating of a diaphragm is generally described by the Bernoulli-Euler Beam Bending Theory [18]. This equation was solved by using the Finite Difference Method (FDM). For the case of a circular and clamped diaphragm with applied a residual stress and incident pressure, the general equation was obtained as:

$$\sigma^{\partial^2 y} \Big/ \partial t^2 = T\nabla^2 y + p_i - p. \tag{1}$$

Where:

$$\nabla^2 y = \frac{\partial^2 y}{\partial r^2} + \frac{1}{r}\frac{\partial y}{\partial r} + \frac{1}{r^2}\frac{\partial^2 y}{\partial \theta^2}. \tag{2}$$

In the above equation p_i is the incidence pressure acting on the diaphragm with a known frequency and p is the pressure increased between the diaphragm and the back plate due to oscillating the diaphragm. All the spatial derivatives have been discretized in a second order manner. To advance the equation in time for simplicity, it is assumed that the diaphragm is at rest with no initial velocity. To model the polarization voltage applied between the diaphragm and the back plate, an analytic equation has been used as in [19]. The electrostatic pressure p_e acting on the diaphragm which causes an initial deflection is equal to:

$$p_e = \frac{1}{2}\varepsilon_0 \left(\frac{E_0}{h_0}\right)^2. \tag{3}$$

The microphone can be modeled as having a piston-like static displacement with an equivalent polarized gap:

$$h^* \approx h_0 - Y_0 \left(1 - \frac{1}{2}\frac{b^2}{a^2}\right) \tag{4}$$

$$Y_0 = \frac{p_e b^2}{4T}\left(1 + 2\ln\frac{a}{b}\right). \tag{5}$$

The response pressure p acting underneath the diaphragm, due to squeezing the fluid between the plates, is not uniform in space so to have the generality of the problem the Reynolds equation has been considered in 2D polar coordinate i.e. r, θ. When the new position of the diaphragm is calculated in each time step the average displacement of the diaphragm is calculated as:

$$y_{ave} = \frac{\int_0^{2\pi}\int_0^a y(r,\theta) r dr d\theta}{\int_0^{2\pi}\int_0^a r dr d\theta}. \tag{6}$$

B. Squeeze Film Analysis

In general, Navier-Stokes equations simulate viscosity, pressure, and inertia in fluid-structure mechanisms. Solving these equations for the geometries containing perforations on the wall requires special schemes and a large number of elements which is a very time consuming progress. These complicated Navier -Stokes equations can be simplified into the Reynolds equation if certain conditions are assumed for the flow. These underlying assumptions are as follows: 1- The air film is isothermal, 2- inertial effects are negligible, 3- amplitude motion and pressure changes are small, 4- fluid velocity normal to the surface is negligible, and 5- the gap is small compared to lateral dimensions $h << 2a$ [20]. Squeeze film analysis simulates the effects of fluid in small gaps between fixed surface and structures moving perpendicular to the surface (Blech [21], Griffin [22], Langlois [23]). Depending on the operating frequencies, the fluid can add stiffening and/or damping to the system [24]. At low frequencies, the fluid can escape before it compresses. Therefore, the fluid only adds damping to the system. At high frequencies, the fluid compresses before it can escape. Therefore, the fluid adds both stiffness and damping to the system. The Reynolds equation for a compressible isothermal gas is given by [25]:

$$12\mu \frac{\partial (hp)}{\partial t} = \nabla.\left(ph^3 \nabla p\right) \tag{7}$$

which it can be shown in cylindrical coordinates as:

$$12\mu h\frac{\partial p}{\partial t} + 12\mu p\left(V_z - u\right) = \frac{h^3 p}{r}\frac{\partial p}{\partial r} + 3h^2 p\frac{\partial p}{\partial r}\frac{\partial h}{\partial r} + h^3\left(\frac{\partial p}{\partial r}\right)^2 + h^3 p\frac{\partial^2 p}{\partial r^2} + \frac{3h^2 p}{r^2}\frac{\partial p}{\partial \theta}\frac{\partial h}{\partial \theta} + \frac{h^3}{r^2}\left(\frac{\partial p}{\partial \theta}\right)^2 + \frac{h^3 p}{r^2}\frac{\partial^2 p}{\partial \theta^2}. \tag{8}$$

In the above given equation $h = h^* + y$ and the term $\partial h / \partial t$ has been replaced by V_z i.e. the normal velocity of the diaphragm and u is the velocity in the holes. A harmonic analysis is used to determine the stiffness and damping effects at high frequencies to model the thin-film fluid behavior between flat surfaces and is based on the Reynolds squeeze film equation known from the Lubrication Theory [26].

The Reynolds squeeze film equations are restricted to structures with lateral dimensions much larger than the gap separation. Furthermore, the pressure change must be small compared to Po, and viscous friction may not cause a significant temperature change.

Adding holes to the back plate will reduce the pressure concentration and will decrease the damping effect in order to control the linear frequency limit of the transducer response. This important term is modeled using the Continuum Theory. The velocity of the flow in the channels with circular cross-section is given by the momentum equation as [27]:

$$\rho\frac{\partial u}{\partial t} = -\frac{\partial p}{\partial z} + \mu\left(\frac{\partial^2 u}{\partial r^2} + \frac{\partial^2 u}{\partial \theta^2} + \frac{1}{r}\frac{\partial u}{\partial r}\right). \tag{9}$$

In the above equation the axial pressure gradient has been replaced by:

$$\frac{\partial p}{\partial z} = \frac{p - p_b}{l_{h,slot}}. \tag{10}$$

Where p_b, is the pressure of the back volume, l_h and l_{slot} are the length of the holes and the slot. This equation is valid only in a fully developed region of the laminar flows in the channels. It is known that when the fluid enters to ducts, it

takes some times that the boundary layers merge together and reach the fully developed condition. This region is called the fully developed length. The laminar entrance length predicted by the Sparrow [28] is:

$$\frac{X_d/D_h}{Re_{D_h}} = 0.0065. \tag{11}$$

To calculate the Re, the mean velocity of the flow must be known. If we assume that the air in the gap moves freely through the openings without compression, the velocity can be scaled as $v_h = h_d/\tau$, where h_d is diaphragm displacement and τ is the time scale of the vibration. Maximum velocity is achieved at high frequencies as $v_h = 1\mu m \times 10kHz = 0.01m/s$. The developing length scale can be calculated as: $X_d = 0.0065 \times \rho \times v_h \times D_h^2/\mu$ so we would have:$X_d \approx 7 \times 10^{-7}$ which is much smaller than the 1% of the openings depth. So it is logical to neglect the developing length and assume that the flow in the holes is in fully developed condition. To apply the holes and the slot effects in the Reynolds and momentum equation, an additional function is introduced as:

$$y_h = \begin{cases} \frac{1}{l_h} & if \ \left(x^2 - x_{hole}^2\right) + \left(y^2 - y_{hole}^2\right) \le R_{hole}^2 \\ \frac{1}{l_{slot}} & if \quad r \ge b \\ 0 & if \quad \text{otherwise} \end{cases} \tag{12}$$

Applying the function $y_h(r,\theta)$ to the momentum equation yields the replacement of a pressure gradient term by: $\partial p/\partial z = (p - p_b) y_h(r,\theta)$. For simplicity the fully developed equation has been descritized in a cylindrical coordinate underneath the diaphragm. To take in to account the holes on the back plate, the velocity over the whole domain except the holes and slot location has been forced to be zero. This is done by multiplying the velocity u in each time step by a function as follows:

$$u(r,\theta) = u(r,\theta) \times \frac{y_h(r,\theta)}{y_h(r,\theta) + \varepsilon}. \tag{13}$$

Where ε, is a small number to avoid dividing by zero.

With this method it is possible to solve the momentum equation for all openings with just one equation.

When the diaphragm moves down, the air inside the back volume compresses slightly. To take this in to account, a new static pressure of the back volume is computed from the ideal gas low and is used as a boundary condition for the diaphragm edge. For the isothermal process we have:

$$\frac{dp_b}{dt} = \frac{\gamma p_{atm}}{\rho V_b} \frac{dm}{dt} \tag{14}$$

$$\frac{dm}{dt} = \int_0^{2\pi} \int_0^R \rho u r dr d\theta. \tag{15}$$

A harmonic analysis is needed to calculate the pressure distribution for the operating frequencies. The pressure distribution can be used to extract the damping and stiffness effects. Because, in this simulation, the Reynolds equation and the diaphragm equation of motion have been coupled and are solved simultaneously, there is no need to calculate the damping and stiffness coefficients. They are specially used when the pressure distribution is known and is needed to find the deflection of the diaphragm based on the given pressure. Thus to simplify the problem, these factors are introduced. This estimation might cause some significant errors on the results if the non-uniform displacement of the diaphragm exists. The main reason for this non-uniformity is due to the existence of the holes on the back plate which causes the non-uniformity of the pressure distribution. So using the average values for the pressure and velocity in these situations some times might not be logical. But after all they are simple to use and can be a good estimation [7]. The phase shift between the pressure and the velocity is caused by compression of the fluid. The average pressure underneath the diaphragm and the average velocity of the diaphragm in each time step can be calculated as:

$$P_{ave} = \frac{\int_0^{2\pi} \int_0^a P_r dr d\theta}{\int_0^{2\pi} \int_0^a r dr d\theta} \tag{16}$$

$$V_{ave} = \frac{\int_0^{2\pi} \int_0^a V_{zr} dr d\theta}{\int_0^{2\pi} \int_0^a r dr d\theta}. \tag{17}$$

TABLE I

FLOW SOLUTION OF NUMERICAL METHOD

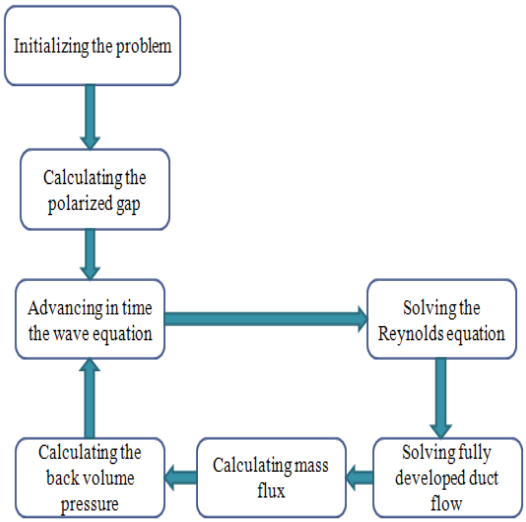

III. NUMERICAL SOLUTION METHOD

Knowing the holes pattern and slot location on the back plate, it is possible to find the function $y_h(r,\theta)$ which is used in the squeeze film and momentum equation. To solve the dynamic equation of motion of the diaphragm with respect to time, it is necessary to solve the Reynolds and momentum equation simultaneously. To do so, when the vibrating equation is advancing in time, the deflection shape of the microphone diaphragm can be determined in each time step, and then the volume between the diaphragm and the back plate is transferred to the subroutine which solves the Reynolds and momentum equation. The flow of the solution is shown in table1. All the equations in the computational domain are discretized in second order manner in spatial and first order in time.

TABLE II
GRID INDEPENDENCY TEST FOR SQUEEZE FILM ANALYSIS IN THREE DIFFERENT MESH SIZES OF 70×120, 80×160, AND 100×190

Pressure contours	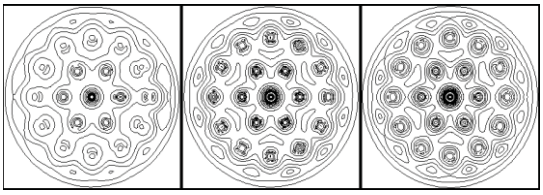		
Average pressure (Pas)	0.2110	0.2059	0.2062

To satisfy the convergence criteria and having the maximum possible time step for Reynolds and momentum equation, the Crank-Nicolson method is implemented [29]. This method is an iterative method to accelerate the convergence speed. The procedure is shown in the equation below:

$$p_{i,j}^{n+1} = \left(Ap_{i+1,j}^{n+1} + Bp_{i-1,j}^{n+1}Cp_{i,j+1}^{n+1} + Dp_{i,j-1}^{n+1}\right) + \left(A' p_{i+1,j}^{n} + B' p_{i-1,j}^{n} + C' p_{i,j+1}^{n} + D' p_{i,j-1}^{n}\right). \tag{18}$$

Descretized form of momentum equation is as below:

$$u_{i,j}^{n+1} = -\frac{1}{\rho} y_{h(i,j)} \left(p_{i,j}^{n+1} - p_b\right) + \frac{\mu}{\rho}\left(Eu_{i,j}^{n} + Fu_{i+1,j}^{n} + Gu_{i-1,j}^{n} + Hu_{i,j+1}^{n} + Iu_{i,j-1}^{n}\right). \tag{19}$$

Where the constants in (18), are related to transformation matrices, the iterations of these equations are done so that the convergence condition is satisfied.

$$\max\left|\frac{p^{n+1} - p^{n}}{p^{n+1}}\right| \le \chi. \tag{20}$$

Where χ is a small value close to zero depending on the accuracy of the solution. Here it is taken into account as 10-6. When the pressure distribution over the back plate is determined in each time step, it is possible to advance the vibration equation in the next time step.

IV. GRID INDEPENDENCY TEST AND CODE ACCURACY

To compare the numerical results for the pressure distribution and the average pressure, the second order numerical code for the solution of vibration equation and Reynolds equation developed in this study is run on the three different meshes of 70 × 120, 80 × 160 and 100 × 190 to study its accuracy and conservative property. The numerical results obtained are shown in Table 2 where the contours are compared in the forgoing three meshes. As it is evident from the table, the numerical results clearly indicate the excellent performance of the grid independency of the codes. All the geometry parameters and the operational condition for comparisons are taken from [30] for a standard microphone type B&K 4146.

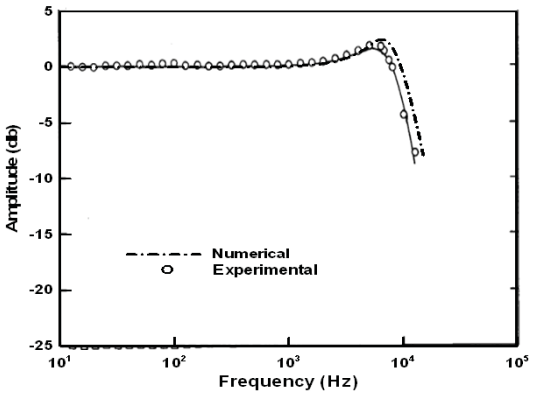

Fig. 1. Comparison of the numerical with experimental results for microphone sensitivity.

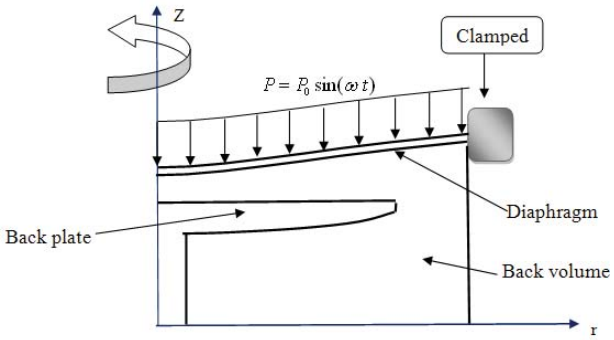

Fig. 2. Geometry of the physical domain.

On the other hand, to check the accuracy of the numerical code, the numerical results obtained for the frequency mechanical response of the microphone is compared with the experimental data which exists in the literature in Fig. 1. As is evident from Fig. 1, the numerical results obtained indicate a very good accuracy of the code.

V. RESULTS AND DISCUSSION

Assuming zero initial velocity of the diaphragm and zero displacement, it is possible to start marching in time. The physical domain shown in Fig. 2 suitably fits the computational domain system i.e. cylindrical coordinate. Also, the finite difference scheme used here can be easily applied due to the availability of uniform orthogonal divisions in the r and θ directions.

It was mentioned that there are three main equations i.e. vibration, Reynolds and momentum equations which need to be solved to get the mechanical response. Before solving the Reynolds equation (to find the pressure distribution) determining the diaphragm deflection is required. To do so, first, the equation of motion of the diaphragm is advanced in time then by knowing the deflection profile and its velocity, it is possible to solve the Reynolds equation for the air layer and the momentum equation for the channels of the back plate.

The schemata of the back plate and its holes are displayed in Fig. 3. In this article, the one hole pattern which has been given from commercial 4146 B&K microphone is studied to

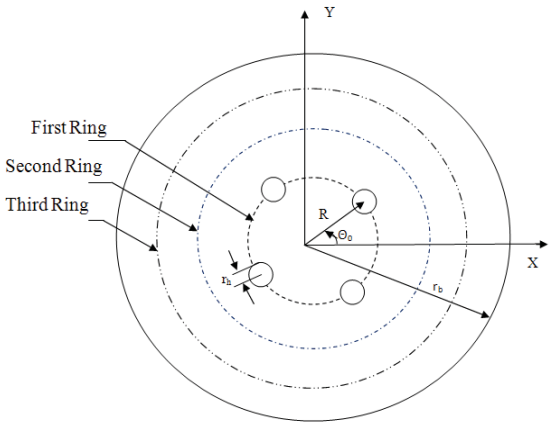

Fig. 3. Schemata of back plate and its holes.

determine its effect on the microphone response. The holes pattern is: (12-6-6-1) in a way that each number in the parentheses shows the number of holes on the specified ring and maximum four rings are considered. It is known that the mechanical performance (i.e. mechanical sensitivity) of a microphone depends on the location of the openings (slot and holes) in the back plate. At a glance, the air layer damping and stiffness effects are a function of the location of the k_{th} opening and the air velocity at the k_{th} opening in the back plate. These values, at any particular opening, depend on the pressure and the acoustic impedance at the opening and can be obtained by solving the Reynolds equation which consists of the acoustic impedance of the slot and holes. As the diaphragm deflection is location-dependent and is not uniform azimuthally, the damping and stiffness (i.e. air flow characteristics) are also dependent on the holes location since the pressure distribution on the back plate surface, including at any openings, is not uniform. Therefore, the location of holes in the back plate does have an important role to play in the damping characteristics.

When the number of holes on the back plate is increased, the average pressure decreases and this is because adding the holes causes the total impedance to decrease so that the core flow can easily move along the holes. In other words, when the diaphragm deflects, the two electrodes get closer to each other and this may compress the air film between them and increase the pressure. Maximum pressure is achieved only if there is no hole on the back plate. This depends on how much decrease of mean pressure is needed to determine how many holes should be applied on the back plate. In low frequency regimes, this air layer does not add much stiffness to the problem because the diaphragm moves slowly, thus the air has adequate time to balance but in high frequencies, due to the high speed of the diaphragm, the air compresses like a spring so that stiffness adds to the problem. In Fig. 4 and Fig. 5 contours of pressure on the back plate for different frequencies have been plotted. All the quantities have been normalized with the mean incidence pressure which acts on the diaphragm. In the first one the pressure distribution is shown when the incidence pressure acting on the diaphragm reaches to its peak value and in the second one the diaphragm deflection is maximum.

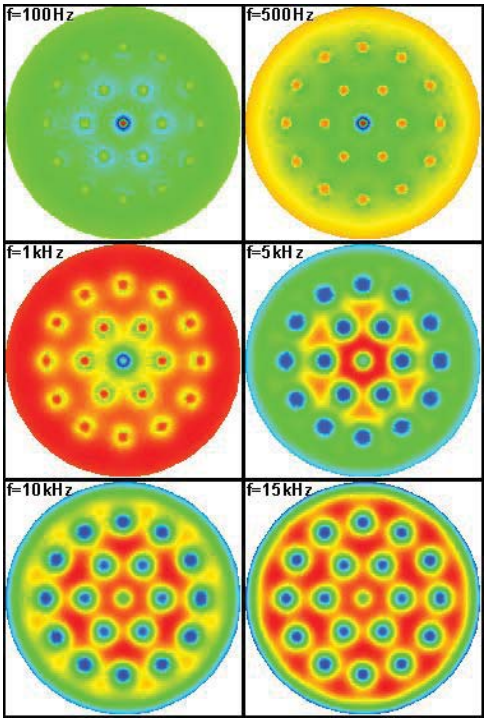

Fig. 4. Contours of pressure on the back for different frequencies (at the peak of incidence pressure).

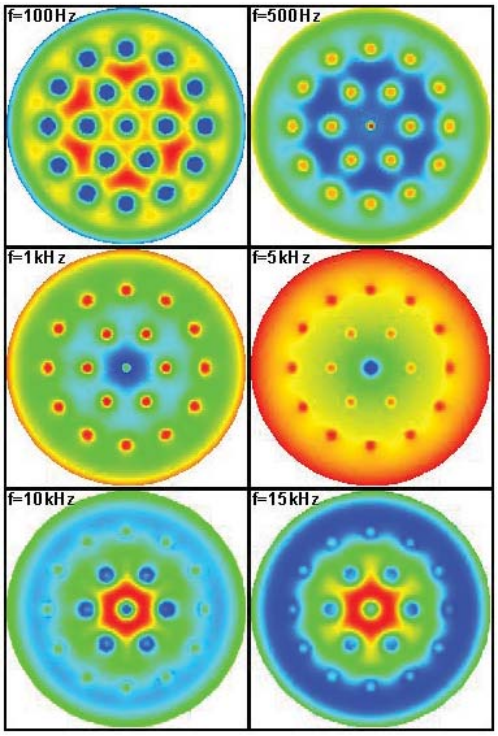

Fig. 5. Contours of pressure on the back for different frequencies (at the peak of diaphragm deflection).

To have a better insight of the problem, the local pressure distribution on the back plate and the holes are shown in Fig. 6 and Fig. 7. In the low frequency regimes where the phase shift is also little, the incidence pressure and the deflection reach their maximum value at the same time but increasing the

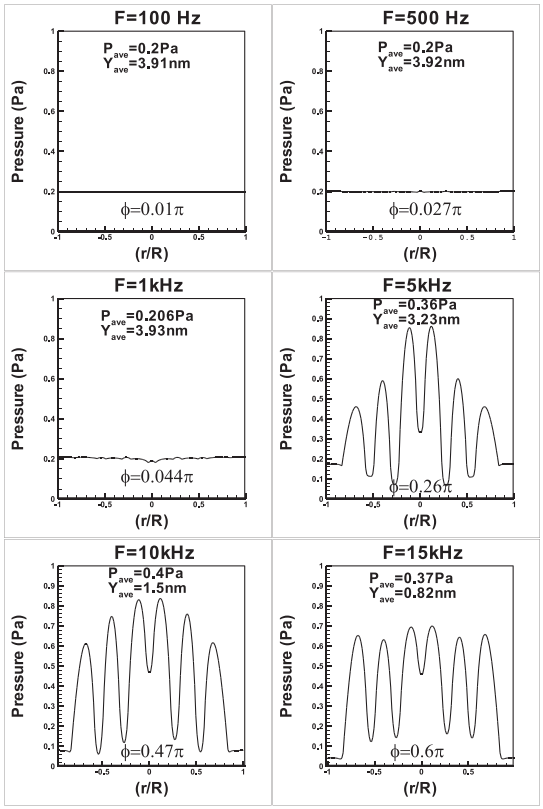

Fig. 6. Local pressure on the back plate for different frequencies (100 Hz), (500 Hz), (1 kHz), (5 kHz), (10 kHz), and (15 kHz) at the peak of incidence pressure.

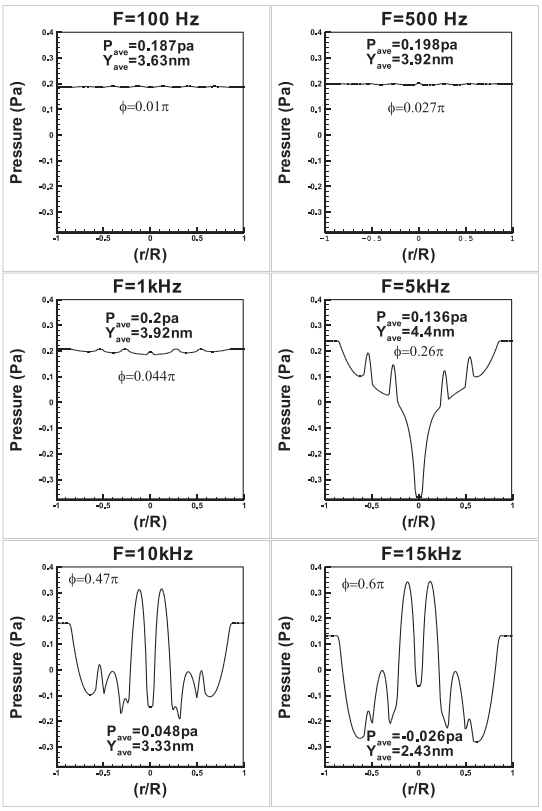

Fig. 7. Local pressure on the back plate for different frequencies (100 Hz), (500 Hz), (1 kHz), (5 kHz), (10 kHz), and (15 kHz) at the peak of diaphragm deflection.

frequency, causes a bigger phase shift. This happens especially near the resonance frequency.

It is clear, as can be seen, that the maximum pressure value for three cases i.e. (100Hz), (500Hz) and (1kHz) are almost the same which are the linear frequency limit for this configuration of the microphone, that's why the pressure value does not change considerably. The upper limit to the operating bandwidth lies close to the vacuum resonant frequency of the diaphragm:

$$f_H = \frac{2.4048}{2\pi a}\left(\frac{T}{\sigma_M}\right)^{1/2} = \frac{2.4048}{2\pi \times 9 \times 10^{-3}}\left(\frac{2000}{4.45 \times 10^{-2}}\right)^{1/2} = 9028 Hz. \tag{21}$$

A large bandwidth is favored by high tension, small diaphragm radius, and low surface mass density (implying a thin diaphragm) but when the role of air damping has been taken to account, this upper limit decreases and, in this case, the resonance frequency comes to about 6 kHz.

To see the effect of air damping on the displacement of the diaphragm, the mechanical response of this microphone configuration has been plotted in Fig. 8 for four air gap i.e. 15, 20, 25 and 30 Micron, respectively.

In the low frequency region, where the speed of the diaphragm deflection is also low, the dominant damping force is due to the deflection of the diaphragm and compressing the

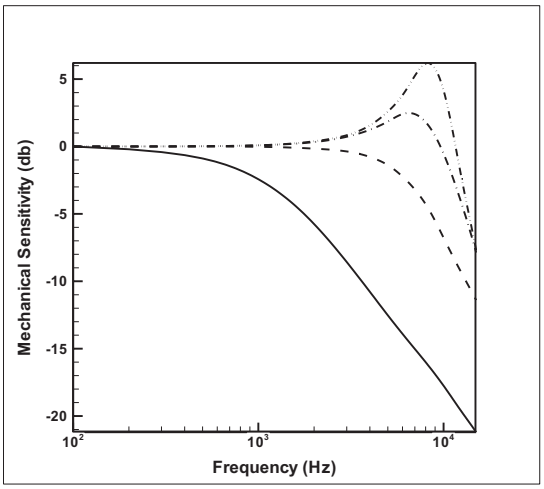

Fig. 8. Mechanical response of the microphone for different air gaps.

back volume air, so that the deflection is almost independent of the air gap and all the plots converge to a constant value. This value depends on the pretension applied to the diaphragm. Decreasing tension will result in large deflection and hence large sensitivity. But it should be noted that this causes the frequency resonance and the operation band width of the microphone to decrease. In high frequency limit, while the speed of the diaphragm is high, the damping force is more significant which limits the amplitude vibration of the

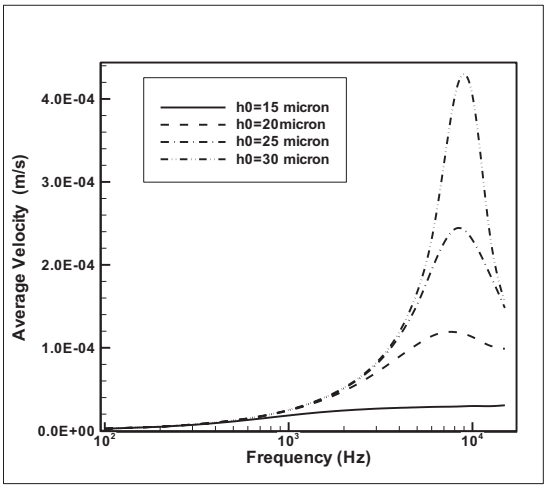

Fig. 9. Average velocity of the diaphragm against the different air gaps.

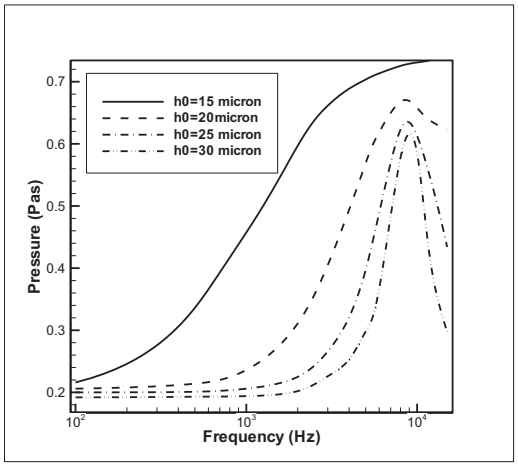

Fig. 10. Average pressure for different air gaps.

diaphragm. This causes the damping of the response in a certain frequency depending on the air pressure which is determined by Reynolds equation.

The average velocity of the diaphragm can be seen in Fig. 9. It is obvious that the velocity of the diaphragm reaches to its maximum near the vacuum resonance frequency. The lowest velocity belongs to smallest air gap and the highest is for biggest air gap. The average pressure in the air gap is plotted in Fig. 10. It can be seen that maximum pressure belongs to the smallest air gap and all of them, except the 15 micron which is critically over damped, have a peak value near the vacuum resonance frequency.

One can see from the Fig. 9 that with the increase in frequency the velocity of the diaphragm is increased, and when it reaches to its maximum value at 9 kHz, it then begins to decrease. This behavior can be seen for the average pressure in Fig. 10. With the increase of the velocity magnitude in the high frequencies, due to lack of enough time for the air to escape within the gap, the air between the electrodes compresses thus the pressure amplitude increases. This increase in pressure does not allow the diaphragm to vibrate freely and thus reduces its amplitude significantly.

With increasing the frequency to 10 kHz and 15 kHz, the deflection value decreases more which means that the diaphragm speed is also low and we have passed the natural resonance frequency.

VI. Conclusion

The viscous damping effect plays an important role in the design of condenser microphones as it dominates the mechanical response of the sensor. In this article a new method is proposed to simulate the response of a condenser microphone. The pressure distribution in the air gap in a transient form can be calculated through the Squeeze Film Theory for any of the desired holes pattern and radius. The effects of the air gap and their pattern on the damping are studied in detail. Vibration of the microphone diaphragm is simulated using the vibration equation to specify the dependence of frequency response of the device to the damping effect. All equations are coupled and solved together in implicit form. The results obtained with this method are in good agreement with the experimental analysis that exists in the literature.

Acknowledgment

The authors would like to thank F. Skoee and H. Shahin, Engineers of the Acoustic Research Center, Granville, OH, for their helpful comments and support and also Dr. H. H. Ghassem sponsor of the Acoustic Research Center for his support and enthusiastic effort to help our research goals.

References

[1] W. Kühnel and G. Hess, "A silicon condenser microphone with structured back plate and silicon nitride membrane," *Sensors Actuat. A: Phys.*, vol. 30, no. 3, pp. 251–258, 1992.

[2] P. R. Scheeper, W. Olthuis, and P. Bergveld, "Improvement of the performance of microphones with a silicon nitride diaphragm and backplate," *Sensors Actuat. A: Phys.*, vol. 40, no. 3, pp. 179–186, 1994.

[3] T. B. Gabrielson, "Mechanical-thermal noise in micromachined acoustic and vibration sensors," *IEEE Trans. Electron Devices*, vol. 40, no. 5, pp. 903–909, May 1993.

[4] T. Veijola and P. Raback, "Methods for solving gas damping problems in perforated microstructures using a 2-D finite-element solver," *Sensors*, vol. 7, no. 7, pp. 1069–1090, 2007.

[5] A. J. Zuckerwar, "Theoretical response of condenser microphone," *J. Acoust. Soc. Amer.*, vol. 64, no. 5, pp. 1278–85, 1978.

[6] C. Tan, Z. Wang, J. Miao, and X. Chen, "A study on the viscous damping effect for diaphragm-based acoustic MEMS applications," *J. Micromech. Microeng.*, vol. 17, no. 11, pp. 2253–2263, 2007.

[7] A. Ranjbar, M. T. Mehrabani, and F. T. Pary, "A numerical study on the viscous damping effect for a condenser microphone," *IEEE Sensors J.*, vol. 11, no. 6, pp. 1307–1316, Jun. 2011.

[8] W. Mclachlan, *Bessel Functions for Engineers*. Oxford, U.K.: Clarendon Press, 1995.

[9] C. Rajalingham, R. B. Bhat, and G. D. Xistris, "Vibration of clamped elliptical plate using exact circular plate modes as shape functions in Rayleigh Ritz method," *Int. J. Mech. Sci.*, vol. 36, no. 3, pp. 231–246, 1994.

[10] J. E. Warren, A. M. Brzezinski, and J. F. Hamilton, "Capacitance-microphone static diaphragm defections," *J. Acoust. Soc. Amer.*, vol. 52, no. 3A, pp. 711–752, 1972.

[11] J. E. Warren, A. M. Brzezinski, and J. F. Hamilton, "Capacitance-microphone static diaphragm defections," *J. Acoust. Soc. Amer.*, vol. 52, no. 5, pp. 711–752, 1972.

[12] S. Hayasaka, "Theoretical investigation of the damping effect of thin fluid films," Electro-Technical Research Laboratory, Tokyo, Japan, Tech. Rep. 467, 1963.

[13] J.-Y. Chen, S.-S. Lee, P. Chang, C.-H. Chu, T. Mukherjee, and G. K. Fedder, "A schematic-based design model for microphone and circuit integration," in *Proc. Microsyst. Packag. Assembly Circuits Technol.*, Oct. 2007, pp. 157–160.

[14] L. Huang, "Viscous flutter of a finite elastic diaphragm in a Poiseuile flow," *J. Fluids Struct.*, vol. 15, no. 7, pp. 1061–1088, 2001.

[15] I. Stiharu and R. B. Bhat, "Vibration of micro plates in electrostatic field using Rayleigh Ritz method," in *Proc. Int. Modal Anal. Conf. Soc. Exper. Mech.*, Orlando, FL, 1997, pp. 765–770.

[16] C. Rajalingham and R. B. Bhat, "Influence of an electric field on diaphragm stability and vibration in a condenser microphone," *J. Sound Vibration*, vol. 211, no. 5, pp. 819–827, 1998.

[17] J.-Y. Chen, Y.-C. Hsu, T. Mukherjee, and G. K. Fedder, "Modeling and simulation of a condenser microphone," in *Proc. Trans. 14th Int. Conf. Solid-State Sensors Actuat. Microsyst.*, Lyon, France, Jun. 2007, pp. 1299–1302.

[18] M.-D. Xue, J. Duan, and Z.-H. Xiang, "Thermally-induced bending-torsion coupling vibration of large scale space structures," *Comput. Mech.*, vol. 40, no. 4, pp. 707–723, 2007.

[19] A. J. Zuckerwar, *AIP Handbook of Condenser Microphone: Theory, Calibration and Measurements*, G. S. K. Wong and T. F. W. Embleton, Eds. New York: AIP, 1995.

[20] Y.-H. Cho, A. P. Pisano, and R. T. Howe, "Viscous damping model for laterally oscillating microstructures," *J. Microelectro Mech. Syst.*, vol. 3, no. 2, pp. 81–87, Jun. 1994.

[21] J. J. Blech, "On isothermal squeeze films," *J. Lubrication Technol.*, vol. 105, no. 4, pp. 615–620, 1983.

[22] W. S. Griffin, H. H. Richardson, and S. Yamanami, "A study of squeeze-film damping," *J. Basic Eng.*, vol. 88, no. 2, pp. 451–456, 1966.

[23] W. E. Langlois, "Isothermal squeeze films," *Quarterly Appl. Math.*, vol. 20, no. 2, pp. 131–150, 1962.

[24] *Squeeze Film Theory*, Ansys, Cannonsburg, PA, Ver. 12.1, 2009.

[25] A. K. Pandey and R. Pratap, "A comparative study of analytical squeeze film damping models in rigid rectangular perforated MEMS structures with experimental results," *Microfluid Nanofluid*, vol. 4, no. 3, pp. 205–218, 2008.

[26] C. E. Brennen, *Hydrodynamics of Pumps, Concepts ETI.*, London, U.K.: Oxford Univ. Press, 1994.

[27] F. M. White, *Viscose Fluid Flow*, 2nd ed. New York: McGraw-Hill, 1991.

[28] A. Bejan, *Convection Heat Transfer*. New York: Wiley, 1984.

[29] K. A. Hoffman and S. T. Chiang, *Computational Fluid Dynamic*, vol. 2, 4th ed. New York: McGraw-Hill, 2000.

[30] A. Zukerwar, "Theoretical response of condenser microphone," *J. Acoust. Sos. Amer.*, vol. 64, pp. 1278–1285, Nov. 1978.

Akbar Ranjbar was born in Tehran, Iran. He received the B.S. degree from the University of Arkansas, Fayetteville, and the M.S. degree from the University of New Orleans, New Orleans, LA, in 1985 and 1987, respectively.

He is currently a Faculty Member with the Electronics Group, Electrical Engineering Department, Engineering College, Shahed University, Tehran. He was one of the Founders of the Engineering College, Shahed University, which was established in 1992. He is also with the Acoustics Laboratories, Shahed University, and Space Research Institute, Tehran. His current research interests include satellite sensors, acoustics sensors and detection devices, and acoustic signal processing with specific interest in instrumentation.

Mohammad Taghi Mehrabani was born in Shahre-Rey, Iran, in 1984. He received the B.S. degree in fluid mechanics engineering from Tabriz University, Tabriz, Iran, in 2006, and the M.S. degree in energy conversion engineering from the Amir Kabir University of Technology (Tehran Polytechnic), Tehran, Iran, in 2008. He is currently pursuing the Ph.D. degree with the Amir Kabir University of Technology.

His current research interests include simulation of heat transfer on complex physical systems and acoustic sensors such as special microphones, magnetohydrodynamics simulation of a plasma opening switch, and fluid flow and heat transfer in eccentric-curved annulus by the aid of the finite-difference time-domain method.

Fatemeh Torkaman Pary was born in Tehran, Iran, in 1980. She received the B.S. degree in applied physics and the M.S. degree in physics (laser optics) from Azad University, Tehran.

She has been with the Acoustic Laboratories, Tehran, since 2005. Her current research interests include condenser microphones and mechanical acoustic sensors.

Ms. Pary is a member of the Acoustic Sensors Group.